The Journal of Supercomputing (2022) 78:6974–6994
https://doi.org/10.1007/s11227-021-04125-4

Automated segmentation of leukocyte from hematological images—a study using various CNN schemes

Seifedine Kadry[1] · Venkatesan Rajinikanth[2] · David Taniar[3] · Robertas Damaševičius[4] · Xiomara Patricia Blanco Valencia[5]

Accepted: 4 October 2021 / Published online: 4 November 2021

Abstract

Medical images play a fundamental role in disease screening, and automated evaluation of these images is widely preferred in hospitals. Recently, Convolutional Neural Network (CNN) supported medical data assessment is widely adopted to inspect a set of medical imaging modalities. Extraction of the leukocyte section from a thin blood smear image is one of the essential procedures during the preliminary disease screening process. The conventional segmentation needs complex/hybrid procedures to extract the necessary section and the results achieved with conventional methods sometime tender poor results. Hence, this research aims to implement the CNN-assisted image segmentation scheme to extract the leukocyte section from the RGB scaled hematological images. The proposed work employs various CNN-based segmentation schemes, such as SegNet, U-Net, and VGG-UNet. We used the images from the *Leukocyte Images for Segmentation and Classification (LISC)* database. In this work, five classes of the leukocytes are considered, and each CNN segmentation scheme is separately implemented and evaluated with the ground-truth image. The experimental outcome of the proposed work confirms that the overall results accomplished with the VGG-UNet are better (Jaccard-Index = 91.5124%, Dice-Coefficient = 94.4080%, and Accuracy = 97.7316%) than those of the SegNet and U-Net schemes Finally, the merit of the proposed scheme is also confirmed using other similar image datasets, such as Blood Cell Count and Detection (BCCD) database and ALL-IDB2. The attained result confirms that the proposed scheme works well on hematological images and offers better performance measure values.

Keywords Hematological images · Leukocyte segmentation · SegNet · U-Net · VGG-UNet · Performance evaluation

✉ Xiomara Patricia Blanco Valencia
xiomarapatricia.blanco@unir.net

Extended author information available on the last page of the article

1 Introduction

As diseases in humans are gradually rising, an automated disease detection system is critically needed, especially when a mass screening process is essential [1–4]. Disease diagnosis with biomedical imaging is often required, in which the disease can be detected with the help of a chosen imaging modality [5, 6]. In the most chronic and infectious disease screening procedures, blood screening is a mandatory procedure, where a blood sample is collected from the patient. Detection of leukocyte (white blood cell) is particularly an essential practice during the screening of infectious diseases. This is normally performed using blood smear images (thin/thick) collected by digital microscopes [7]. Normally, hematological images collected using prescribed clinical protocol show vital information about the health condition of the patient. Further, assessment of the leukocyte count per micro-liter is also an approved practice to verify the health condition and to check the immunity level.

This work aims to develop an automated segmentation system to extract various classes of the leukocyte images available in the clinical-grade hematological test images. In the literature, a number of semi-automated/automated image processing actions have been proposed, which examined leukocyte from thin blood smear images. Our work aims to use the Convolutional Neural Network (CNN) supported segmented scheme to extract the leukocyte section with better segmentation accuracy. In the literature, a number of pre-trained and customary CNN segmentation schemes are available, which examine biomedical images recorded using varied imaging modalities [8–12]. The development of a customary CNN scheme for a chosen image is computationally complex, and hence, pre-trained CNN designs are extensively adopted by most researchers due to its availability, performance, and adaptability toward varied imaging modalities [13–17].

In this research, we adopted well-known CNN schemes, such as SegNet [9, 10], U-Net [11–13], and VGG-UNet [14–17], to extract leukocyte fragments from images with enhanced accuracy. After extracting the leukocyte fragment, a relative assessment between the extracted section and the available Ground-Truth (GT) is done to confirm the performance of the CNN scheme. The test images used in this proposed research are collected from *Leukocyte Images for Segmentation and Classification (LISC)* dataset [18].

This dataset consists of the five classes of leukocyte images with a dimension of 720*x*576*x*3 pixels. LISC database comprised of 376 images in which 250 images are available with GT, and the remaining 126 images are without the GT. During the experimental evaluation, each image is resized into 256*x*256*x*3 pixels and then the image augmentation is implemented during the training of the CNN. After the training, the performance of the CNN segmentation scheme is tested using the 250 images, which are available with the GT. The experimental investigation is separately implemented with SegNet, U-Net, and VGG-UNet. The extracted leukocyte fragment is then compared with the GT. We also calculate the Image Performance Measures (IPM), and based on these values, the performance of the CNN segmentation schemes is validated. The experimental

outcome confirms that the CNN scheme is a promising automated segmentation technique. After pre-tuning, the VGG-UNet scheme offered a better outcome compared to SegNet and U-Net. The performance of the proposed scheme is then confirmed and validated using similar medical images existing in the literature, such as Blood Cell Count and Detection (BCCD) database and ALL-IDB2. For every image cases, the proposed scheme helps to get better segmentation accuracy and this confirms that the proposed scheme works well for hematological images. The main contribution of this research work is: (1) Employing the pre-trained CNN segmentation technique to extract the abnormal section from the test image and (2) Performance evaluation of the proposed scheme on well-known benchmark images.

The remaining sections of this work are structured as follows: Sect. 2 describes the related work, Sect. 3 explains the adopted methodology, Sects. 4 and 5 present the results and conclusion of this research, respectively.

2 Related work

Blood screening is a commonly adopted disease prescreening procedure, and the assessment of leukocyte type and its count is also an essential practice in clinical level assessment. Due to its significance, a considerable number of leukocyte examination procedures are proposed and implemented in the literature. Table 1 presents a summary of various image processing procedures implemented to examine the hematological images.

Table 1 presents the few recently implemented leukocyte segmentation technique using traditional and DNN-based techniques. A short review of the segmentation technique employed to extract the White Blood Cell (WBC) can be found in the work of Sapna and Renuka [31]. All this work confirms that the extraction and evaluation of the WBC is a significant task during the blood level disease detection and to reduce the diagnostic burden, it is necessary to employ an automated WBC evaluation system. The recent works in the literature confirms that the CNN approaches help to achieve a superior result during the data assessment [32–35]. Hence, this research aims in implementing the CNN supported scheme to assess the considered database. An automated hematological image examination scheme should have the capability to detect/classify the leukocyte (WBC) with better accuracy. To achieve an automated detection, this research work employed the pre-trained CNN scheme available in the literature, and the performance of the considered CNN network is then confirmed with an experimental study using the benchmark LISC database.

3 Methodology

This section describes the proposed scheme, the image database used as a benchmark, the adopted CNN schemes, as well as the performance measures.

Table 1 Summary of recent leukocyte segmentation techniques for hematological images

References	Image processing technique employed to examine the hematological images	Database	Outcome (%)
Rezatofighi et al. [19]	This work introduced the LISC dataset and implements a classification scheme based on the Local Binary Pattern (LBP) and other texture features	LISC	An overall accuracy of 96 is achieved
Rezatofighi and Soltanian-Zadeh [20]	This work implements a machine learning scheme using textural feature based classification of the various leukocyte sections	LISC	Provided an overall accuracy of 96 with SVM classifier
Alam and Islam [21]	Leukocyte detection using You Only Look Once (YOLO) scheme is employed and its performance is validated with other existing Deep-Neural-Network (DNN) schemes	BCCD	Accuracy attained YOLO: 86.89 VGG16:100 ResNet50: 95.08 InceptionV3:100 MobileNet: 93.44
Vatathanavaro et al. [22]	Leukocyte classification using VGG-16 and ResNEt50 is implemented	BCCD & LISC	Validation accuracy VGG16 = 72.07 ResNet50 = 88.29
Jung et al. [23]	A CNN scheme called W-Net is developed to extract and evacuate the leukocyte segment	LISC	Average classification accuracy = 96.00
Prinyakupt and Pluempitiwiriyawej [24]	Morphological segmentation and classification of leukocyte is employed	Private dataset	Linear model outcome Accuracy = 98.7 Sensitivity = 98.1 Specificity = 99.5 Precision = 89.2 Naïve Bayes model outcome Accuracy = 97.3 Sensitivity = 96 Specificity = 98.8 Precision = 80.6

Table 1 (continued)

References	Image processing technique employed to examine the hematological images	Database	Outcome (%)
Almezhghwi, and Serte [25]	Leukocyte classification is implemented using DNN with tenfold cross-validation	LISC	Validation accuracy VGG16 = 95.7 VGG19 = 95.9 ResNet18 = 95.4 ResNet50 = 97.4 ResNet121 = 98.3 ResNet169 = 98.8
Li and Wu [26]	Detection of leukocyte using YOLOv3 is implemented	LISC	Validation accuracy YOLOv3 = 91.5 Improved-YOLOv3 = 96.4
Kutlu et al. [27]	DNN based leukocyte classification is implemented	BCCD & LISC	Validation accuracy AlexNet = 97 VGG16:97 GoogleNet = 96 ResNet50 = 97
Dey et al. [28]	Implementation of hybrid segmentation technique is achieved using Shannon's entropy based Chan-Vese technique	LISC	Performance measures Accuracy = 99.52 Precision = 93.85 Sensitivity = 94.03 Specificity = 99.19 F1-Score = 98.28
Raja et al. [29]	Leukocyte segmentation is achieved using Shannon's entropy and Level-Set technique	LISC	Performance measures Accuracy = 98.14 Precision = 94.62 Sensitivity = 90.28 Specificity = 97.63 F1-Score = 96.24

Table 1 (continued)

References	Image processing technique employed to examine the hematological images	Database	Outcome (%)
Rajinikanth et al. [30]	Hough transform-based leukocyte segmentation procedures are implemented and the outcome is evaluated against the GT. The eminence of this technique is compared and validated with other semi-automated segmentation practice available in the literature	LISC	Performance measures Accuracy = 97.96 Precision = 94.68 Sensitivity = 91.42 Specificity = 98.41 F1-Score = 97.28

3.1 Proposed scheme

The structure of the proposed scheme and its stages are depicted in Fig. 1. Initially, the essential test images are gathered from the LISC database. All the RGB images of the LISC database are resized to 256*x*256*x*3 pixels to reduce the computation complexity. The existing pre-trained CNN schemes, such as SegNet, U-Net, and VGG-UNet, are then used to extract the important fragment from the test images. The chosen CNN scheme is trained using the existing LISC dataset images and during this task, image augmentation, such as flip and rotate is used to increase the learning capability of the CNN. After the training process is completed, the original LISC images along with the GT (250 images) are then used to test the performance of the CNN. After image segmentation, the binary version of the segmented image is considered as the outcome and finally, this image is compared against its related GT. The results from the CNN are also compared with results from the existing literatures.

3.2 Image database

The development of an appropriate disease detection system is essential in the medical domain. Validating the system with the clinical-grade benchmark images is also critical. In this research, we use the LISC dataset, which is one of the clinical-grade leukocyte image datasets, developed in the year 2010 by Rezatofighi et al. [19]. This dataset consists of five categories of images, namely basophil, eosinophil, lymphocyte, monocyte, and neutrophil, as well as mixed cases. All

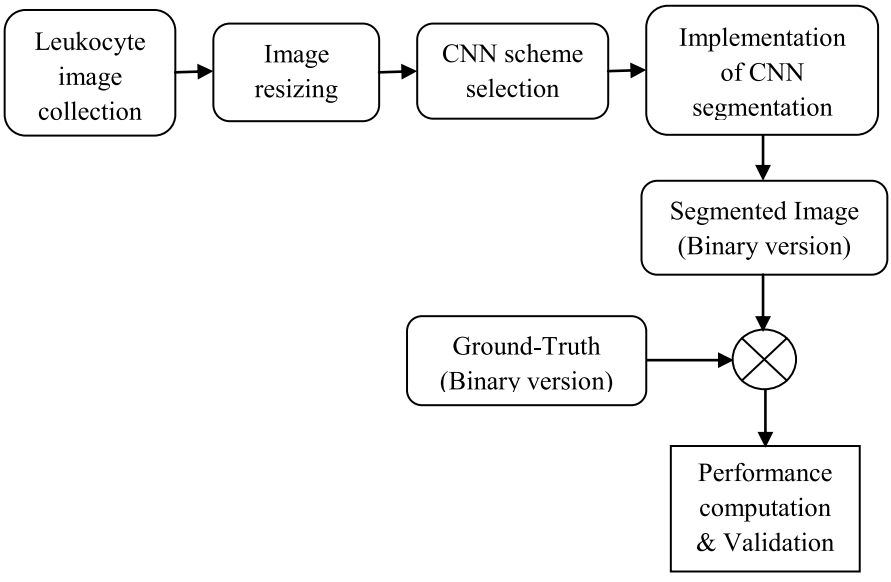

Fig. 1 Structure of the proposed CNN segmentation scheme

these images are associated with the GT, and this dataset also has 126 images without the GT. Other related information, such as patient-related details, can be accessed from [18–20]. Figure 2 illustrates a sample test imagery of LISC with different classes.

Along with the LISC images, this research work also considers Blood Cell Count and Detection (BCCD) database [36] and ALL-IDB2 [37–39] to test the performance of the proposed scheme and the sample images from this database are depicted in Fig. 3. In this work, 250 images from each database is considered to validate the performance of the employed segmentation system.

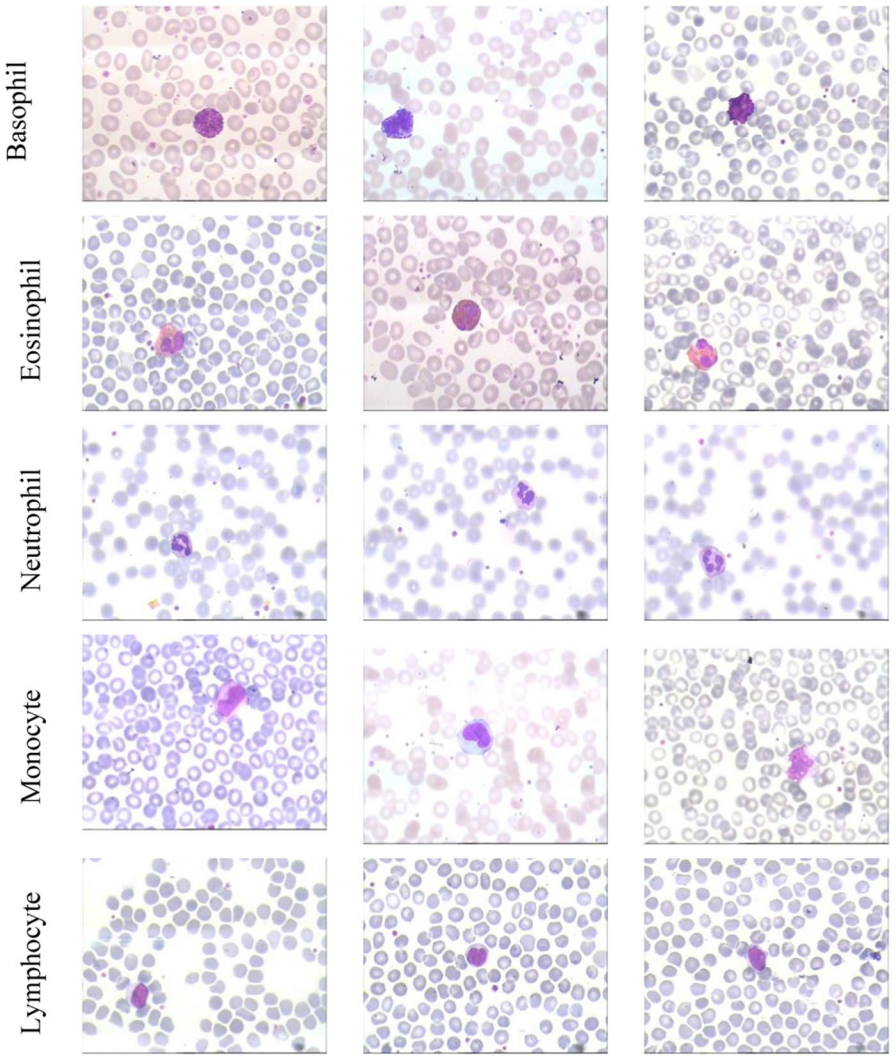

Fig. 2 Sample test images available in the LISC database

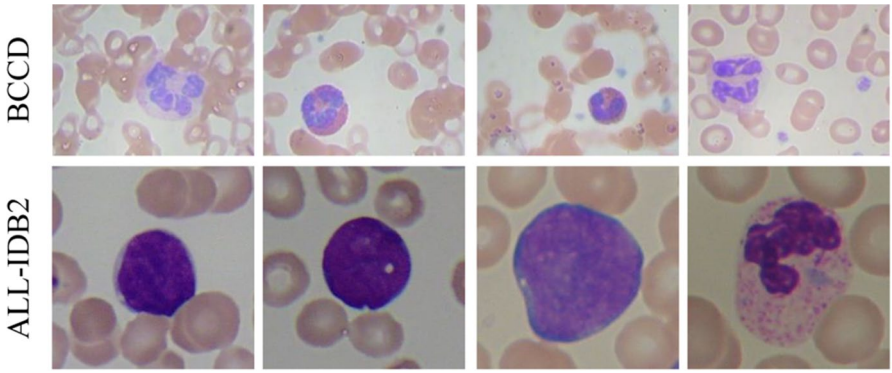

Fig. 3 Sample images of Leukocyte data considered for validation

3.3 CNN scheme

During the medical image diagnosis, the commonly performed image processing procedures are segmentation and classification. During the segmentation task, the essential image section (Region-Of-Interest) is extracted using a chosen technique and is then evaluated using a chosen computer algorithm to detect the disease. The development of accurate image segmentation is always essential to get better disease detection accuracy.

In the literature, a significant amount of traditional [30, 40, 41] and modern (CNN) [9, 11, 42, 43] medical segmentation techniques have been used. Implementation of the traditional segmentation techniques is time consuming, and most of the existing traditional techniques are semi-automated methods and frequently need operator assistance. Due to this reason, modern techniques are widely preferred to examine medical images of varied modalities. Recently, pre-trained CNN schemes have been extensively adopted in the image processing domain, in which the pre-trained CNN schemes work well on a class of images with varied dimensions. Further, the trained CNN on a particular image case will produce better results compared to the traditional approaches. In this work, the CNN schemes, such as SegNet, U-Net, and VGG-UNet are considered to examine the LISC images. These CNN schemes are initially trained with the images of the LISC. During this process, the original as well as the augmented images are considered. After the training, the performance of the CNN is tested and validated using the leukocyte images available with the GT.

3.3.1 SegNet

SegNet is a well-known CNN scheme proposed in 2015. This scheme is widely used to implement the pixel-wise analysis of RGB/gray-scale images [9–11].

The SegNet is constructed by implementing a series of structured Convolutional Encoder-Decoder (CED) framework, and every framework transfers the learned

information to the next successive section. The structure of the traditional SegNet is depicted in Fig. 4. In the implementation, we used the following parameters: image augmentation is fixed as linear, learning rate is assigned as 0.005, decoder-encoder batch size is fixed as 4, normal weight initialization, linear dropout rate and Stochastic Gradient Descent (SGD) adaptive learning rate is considered. The last layer of this scheme is equipped with a Sigmoid activation that provides a classified binary image (which groups the pixel into two groups, such as the Leukocyte section and background). The final outcome of the SegNet is converted into a binary image in order to compare it with the binary GT.

3.3.2 U-Net

U-Net was proposed in 2015 as a sliding window convolutional network, dedicatedly developed to examine test images of the ISIC challenge database [12]. In recent years, due to its performance and significance, a considerable number of modified versions of U-Net schemes are available for other image databases [13–16].

The U-Net scheme used in this research is adopted from the work of El Adoui et al. [11], and the architecture is presented in Fig. 5. Here, the test image and the segmented image have the dimension of $256x256x3$ pixels. The initial tuning of the U-Net is the same as those for the SegNet, and are similar for the VGG-UNet scheme. The working methodology is also similar to the conventional encoder-decoder scheme. Finally, the classifier unit helps to get the outcome with two class image pixels grouped as the binary image. Other related information on the conventional U-Net can be found in [13–17].

3.3.3 VGG-UNet

A substantial number of CNN segmentation schemes are available in the literature, and the VGG-UNet is one of the enhanced forms of the U-Net scheme. The working

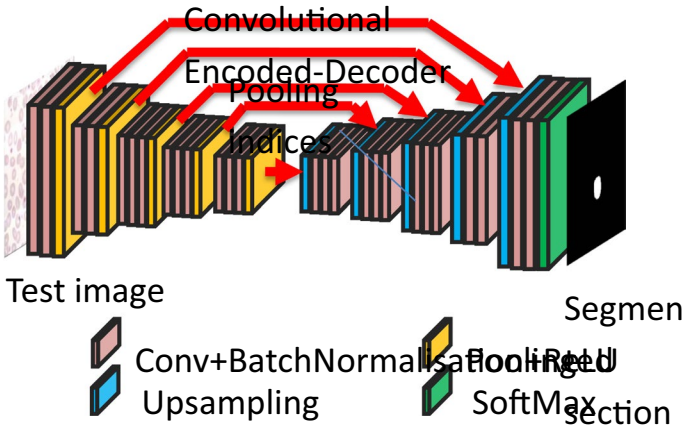

Fig. 4 Structure of the SegNet scheme

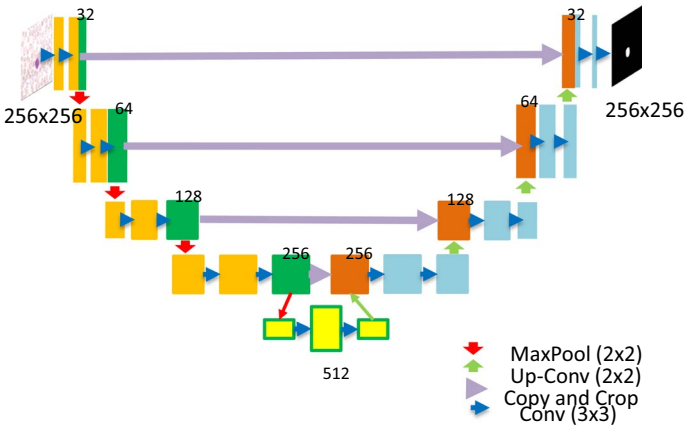

Fig. 5 Structure of the U-Net scheme

parameters and the pre-tuning of the VGG-UNet are similar to the U-Net, and in this approach, the learned features of the VGG16 scheme is considered to enhance the segmentation accuracy. During the implementation, all the examination images are resized into $224x224x3$ pixels. The binary image produced by this scheme is resized into $256x256x1$ to have a fair comparison with the other CNN segmentation methods. In this work, the Convolutional part of the VGG16 will act as the encoder part and the Up-Convolutional part of the U-Net act as the decoder part. Finally, the Sigmoid activation helps to get the segmented result. Other information related to the VGG-UNet can be found in the following work [13–17].

3.4 Performance measures

CNN segmentation performance needs to be authenticated by calculating the image performance values. After extracting the leukocyte segment from the chosen hematological image, a relative assessment with the existing GT is then performed and the essential values of the performance measures, such as Jaccard-Index (JI), Dice-Coefficient (DC), Accuracy (AC), Precision (PR), Sensitivity (SE), Specificity (SP), and Negative-Predicted-Value (NPV), are calculated. Based on these values, the performance of the SegNet, U-Net, and VGG-UNet is validated. This comparison uses the binary images, in which the leukocyte region is considered as Positive (P) pixel (binary1) and the background section is accounted as Negative (N) pixel (binary0). This comparison helps to compute the measures depicted in Eqs. (1) to (9) [45–48].

$$FP_{\text{rate}} = FP/N = FP/(TN + FP) \tag{1}$$

$$FN_{\text{rate}} = FN/P = FN/(TP + FN) \tag{2}$$

$$JI = F1 - Score = TP/(TP + FP + FN) \tag{3}$$

$$DC = 2TP/(2TP + FP + FN) \tag{4}$$

$$AC = (TP + TN)/(TP + TN + FP + FN) \tag{5}$$

$$PR = TP/(TP + FP) \tag{6}$$

$$SE = TP_{\text{rate}} = TP/P = TP/(TP + FN \tag{7}$$

$$SP = TN_{\text{rate}} = TN/N = TN/(\text{TN} + \text{FP}) \tag{8}$$

$$NPV = TN/(TN + FN) \tag{9}$$

where *TN*, *TP*, *FN,* and *FP* represent true-negative, true-positive, false-negative, and false-positive, respectively.

4 Results and discussion

After image resizing and CNN pre-tuning with the LISC dataset, the proposed segmentation is initially implemented using the test images with the GT. Figure 6 depicts the sample test image (Basophil class). Figure 6a, b represent the resized examination image and the related GT, respectively. Figure 6c depicts the saliency map generated by CNN during the learning process, and Fig. 6d shows the extracted binary image with the SegNet scheme. The saliency map clearly shows that CNN precisely identified the section (leukocyte) to be extracted by the final Sigmoid activation function. A similar procedure is then repeated using U-Net and VGG-UNet schemes. Their results are depicted in Fig. 6e, f, respectively. From these images, it is clearly seen that, when the CNN is perfectly trained with the considered image database, it identifies and segments the leukocyte section with better accuracy.

After mining the leukocyte, a number of measurements using Eqs. (1) to (9) are computed. The comparison results between Fig. 6b, d–f are shown in Tables 2 and 3. The performance measure obtained by SegNet is shown to be better than those by U-Net and the VGG-UNet. The process is then replicated to all LISC images.

The LISC dataset also consists of some complex hematological images which are challenging to many proposed computer-assisted disease detection tools, as these images are associated with more than one leukocyte section. Figure 7 shows the images with two and three leukocyte sections in a single image frame.

Figure 6 shows the image and the GT, as well as the saliency map by the SegNet scheme. The saliency map clearly confirms the correctness of the pre-training procedure implemented on the CNN segmentation using the LISC dataset. Due to its initial training, the CNN architecture will remember the pixel groups belong to the leukocyte section and efficiently recognizes all the pixels to be extracted. From the

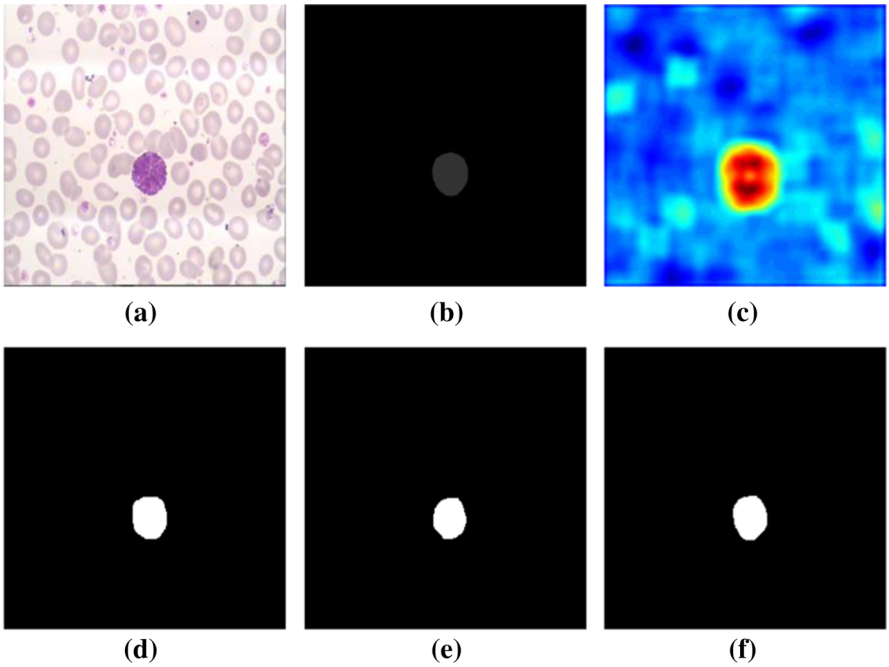

Fig. 6 Sample results using Basophil class test image Test image, **b** GT, **c** Saliency map, **d–f** shows extracted Leukocyte image using SegNet, U-Net, and VGG-UNet, respectively

Table 2 Performance values for the extracted leukocyte with GT

CNN scheme	Pixel level image comparison				FP rate	FN rate
	TP	FP	TN	FN		
SegNet	997	87	64,445	7	0.0013	0.0070
U-Net	884	200	64,449	3	0.0031	0.0034
VGG-UNet	970	114	64,441	11	0.0018	0.0112

Table 3 Essential performance values computed using leukocyte and GT comparison

CNN scheme	Performance measures (%)						
	JI	DC (F1-score)	AC	PR	SE (TP rate)	SP (TN rate)	NPV
SegNet	91.3841	95.4981	99.8566	91.9742	99.3028	99.8652	99.9891
U-Net	81.3247	89.7007	99.6902	81.5498	99.6618	99.6906	99.9953
VGG-UNet	88.5845	93.9467	99.8093	89.4834	98.8787	99.8234	99.9829

saliency map, it is clear that the enhanced pixels belong to the leukocyte section, which will be identified and extracted by the final pixel classification layer. Approximately, similar results are obtained by both U-Net and VGG-UNet.

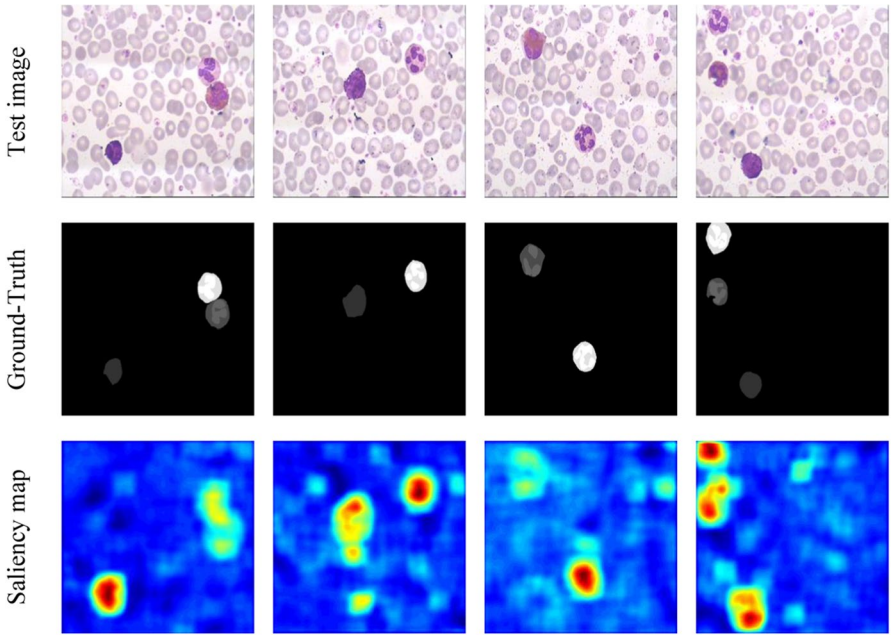

Fig. 7 Results for complex blood smear images

CNN segmentation technique is applied to the entire LISC dataset, which has the GT. The results for each leukocyte class are presented in Table 4. From this table, it is clear that SegNet, U-Net, and VGG-UNet successfully produce good image performance measures when compared with the GT, and this demonstrates that the abilities of CNN segmentation schemes.

To identify the overall performance measure, the average performance measure for each CNN scheme is separately computed. The overall measure is then compared using the Glyph-Plot [36] as shown in Fig. 8. This figure verifies that the overall performance by VGG-UNet is better compared to SegNet and U-Net. Compared to the SegNet, the traditional U-Net showed poor performance. This performance can be improved by varying the initial parameters of the pre-trained U-Net architecture.

The results obtained from this study confirm that the CNN schemes are automated schemes and work well on the leukocyte images with varied classes. Further, the overall performance measures, such as JI, DC, AC, PR, SE, SP, and NPV show promising results on each segmentation scheme.

The results of the proposed research are also evaluated against the existing semi-automated and hybrid image segmentation procedures available in the literature, and the results are presented in Figs. 9 and 10.

Figure 9 depicts the performance evaluation with Basophil image class and the results obtained by the Chan-Vese segmentation [28] technique and the CNN scheme. The Chan-Vese segmentation is used after the image thresholding process. The overall performance measure is approximately similar to the results of VGG-UNet.

Table 4 Performance measures of individual leukocyte image class

Image class	CNN scheme	Performance measures (%)						
		JI	DC (F1-Score)	AC	PR	SE (TP rate)	SP (TN rate)	NPV
Basophil	SegNet	92.0752	95.5517	97.9053	91.6841	99.2074	99.1653	99.9064
	U-Net	91.0826	94.2281	97.5634	90.8058	99.2155	99.3106	99.9162
	VGG-UNet	92.0452	95.0736	98.7992	91.2545	98.9551	99.3875	99.9131
Eosinophil	SegNet	90.3175	93.0636	96.7395	91.7726	98.6185	98.3073	98.7716
	U-Net	91.0636	93.7743	96.8116	91.0736	98.3173	98.1843	98.2284
	VGG-UNet	90.8072	93.3327	97.1678	91.6194	98.2844	98.2005	98.6185
Neutrophil	SegNet	91.3318	94.9174	97.7538	92.1073	98.9743	98.7436	99.2254
	U-Net	90.5732	93.8636	96.9575	91.4974	98.6639	98.2974	99.3006
	VGG-UNet	91.2265	94.1864	97.6937	92.0865	98.6694	98.8143	99.5495
Monocyte	SegNet	91.4926	94.8025	97.4953	91.2286	98.7453	98.7714	99.3926
	U-Net	92.1107	94.6186	97.2064	91.0375	98.1535	98.3372	99.6247
	VGG-UNet	92.2215	94.8946	97.5927	91.5517	98.4738	98.8225	99.3279
Lympho-cyte	SegNet	90.7946	93.1667	97.4426	91.1744	98.9427	98.4227	98.4812
	U-Net	91.1146	93.7268	96.8852	91.0648	98.3372	98.5924	98.4480
	VGG-UNet	91.2615	94.5528	97.4047	91.3163	98.4074	98.3155	98.3957
Average	SegNet	91.2023	94.3004	97.4673	91.5934	98.8976	98.6821	99.1554
	U-Net	91.1889	94.0423	97.0848	91.0958	98.5375	98.5444	99.1036
	VGG-UNet	91.5124	94.4080	97.7316	91.5657	98.5580	98.7081	99.1609

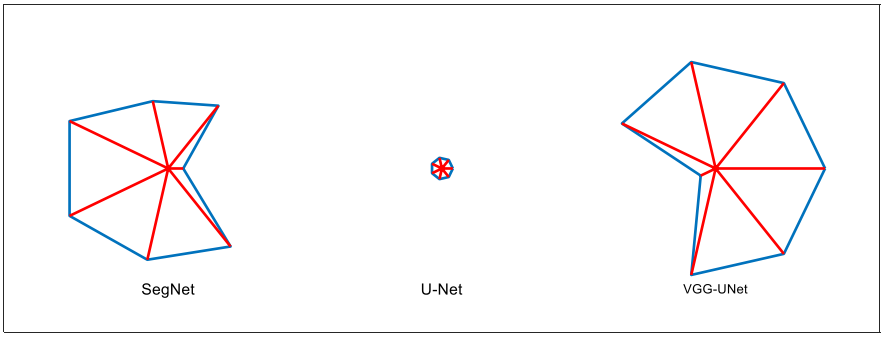

Fig. 8 Glyph-plot demonstrating the overall performance measure

Figure 10 presents a comparison result between the earlier works performed on the LISC database, such as Chan-Vese [28], Level set [29], and Hough transform [30] with proposed VGG-UNet. The earlier works discussed in the literature [28–30] are hybrid image processing methods, in which the preprocessing is performed using a heuristic algorithm-assisted thresholding procedure, and mining is employed with the chosen segmentation technique. The overall accuracy by the VGG-UNet is

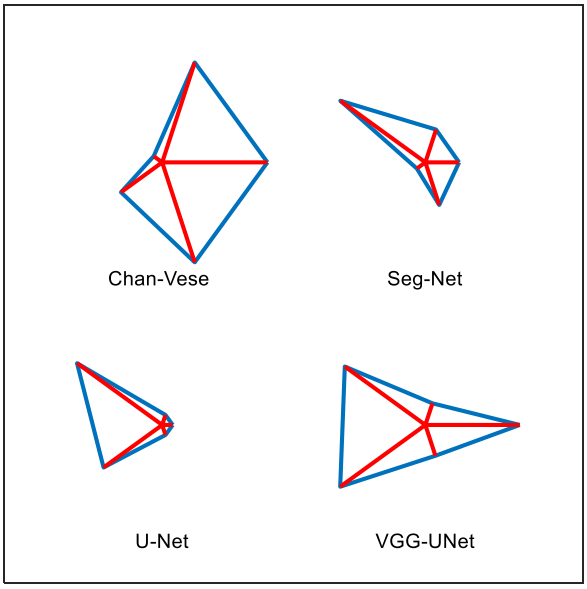

Fig. 9 Glyph-Plot of the overall performance measures obtained with Basophil image class

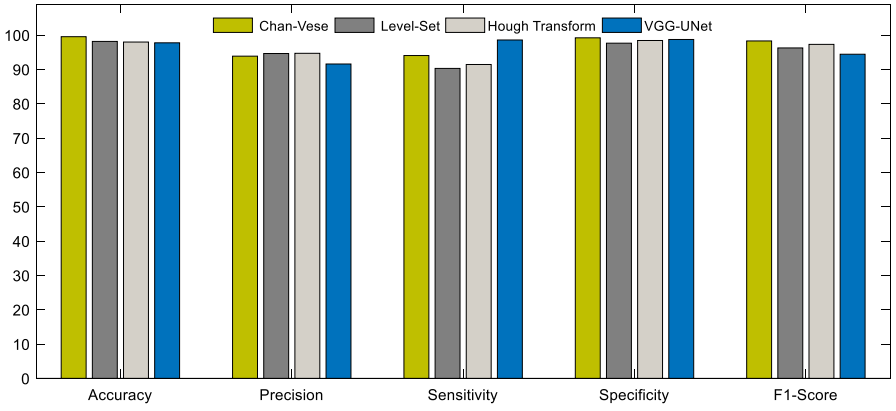

Fig. 10 Performance evaluation between VGG-UNet with existing semi-automated and hybrid image processing schemes

quite similar to that of the existing methods, and sensitivity and specificity are better compared to the existing traditional procedures.

Figure 11 presents the sample results achieved with VGG-UNet, and this result confirms that the outcome in both BCCD and ALL-IDB2 database is good. This result is compared with the segmentation result of VGG-SegNet, and the outcome is presented in Fig. 12. From this figure, it can be noted that, the VGG-UNet based segmentation helps to get a better average values of JI, DC, and AC compared to

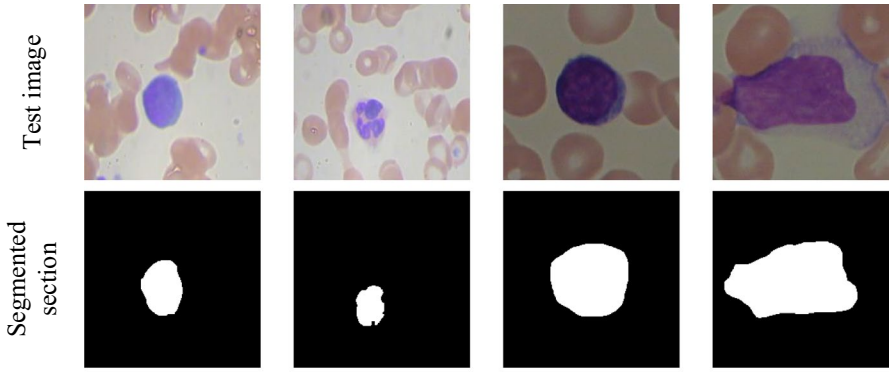

Fig. 11 Results achieved with BCCD and ALL-IDB2

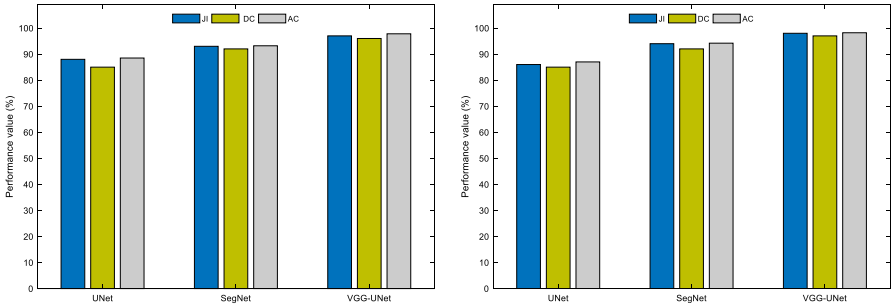

(a) Results for BCCD **(b)** Results for ALL-IDB2

Fig. 12 Comparison of average performance achieved for 250 images

UNet, SegNet, and VGG-SegNet. Figure 12a presents the BCCD database outcome, and Fig. 12b shows the ALL-IDB2 image result. These results confirm that the VGG-UNet helps to get a comparatively better outcome on both the datasets.

The future scope of our research work may be concentrated toward improving the performance of the CNN schemes by adjusting the initial parameters, such as adjusting the image augmentation process, improving the learning, modifying the decoder-encoder batch, adjusting the weight initialization process, modifying the dropout rate, and modifying the activation layer.

This work employed encoder-decoder (VGG-UNet) scheme to achieve accurate segmentation of the leukocyte region in RGB-scaled image. The outcome of the encoder section will be the learned features (Deep-Features), and this feature can be considered to classify the images using a binary or multiclass classifiers. The future scope of this research includes: (1) Implementation of VGG supported automated image classification, (2) Development of VGG-SegNet, and (3) Examination of clinical-grade images.

5 Conclusion

Due to its medical importance, a significant amount of image assessment schemes is planned and implemented by the researches for the medical images with varied modalities. This research presented and automated leukocyte extraction system from hematological images using the benchmark LISC dataset. This work used the pre-trained CNN segmentation procedures, such as SegNet, U-Net, and VGG-UNet to extort the leukocyte section with better accuracy. The proposed segmentation procedure is implemented on 250 images associated with the GT and before implementing the segmentation process, every test image is resized into $256x256x3$ pixels, in order to reduce the computation burden. The results are then compared to identify which CNN scheme produced the best outcome for the LISC dataset. Our experimental results show that the VGG-UNet produced better results than SegNet and U-Net. The outcome of the VGG-UNet is also authenticated against the other hybrid segmentation procedures existing in the literature. Further, the eminence of proposed scheme is tested and validated on BCCD and ALL-IDB2 and these results also verify that this technique helps to segment the leukocyte image perfectly. This research work demonstrated that CNN is useful and is significant in the clinical domain. In future, we will examine the clinical grade of hematological images. Furthermore, the proposed VGG-UNet approach can also be considered to classify the considered image database with a binary and multiclass classifier to support the automated leukocyte class recognition.

References

1. Fernandes SL, Rajinikanth V, Kadry S (2019) A hybrid framework to evaluate breast abnormality using infrared thermal images. IEEE Con Electron Mag 8(5):31–36. https://doi.org/10.1109/MCE.2019.2923926
2. Fernandes SL, Tanik UJ, Rajinikanth V, Karthik KA (2019) A reliable framework for accurate brain image examination and treatment planning based on early diagnosis support for clinicians. Neural Comput Appl. https://doi.org/10.1007/s00521-019-04369-5
3. Ahilan A, Chandra Babu G, Senthil Murugan N, Parthasarathy MG, Raja C, Kadry S, Kumar SN, Agees Kumar C, Jarin T, Krishnamoorthy S, Malarvizhi Kumar P (2019) Segmentation by fractional order Darwinian particle swarm optimization based multilevel thresholding and improved lossless prediction based compression algorithm for medical images. IEEE Access 7:89570–89580. https://doi.org/10.1109/ACCESS.2019.2891632

4. Hussain UN, Khan MA, LaliI U, Javed K, Ashraf I, Tariq J et al (2020) A unified design of ACO and skewness based brain tumor segmentation and classification from MRI scans. Control Eng Appl Inform 22(2):43–55
5. Bakiya A, Kamalanand K, Rajinikanth V, Nayak RS, Kadry S (2020) Deep neural network assisted diagnosis of time-frequency transformed electromyograms. Multimedia Tool Appl 79(15–16):11051–11067. https://doi.org/10.1007/s11042-018-6561-9
6. Kadry S (2020) An efficient apriori algorithm for frequent pattern mining using mapreduce in healthcare data. BullElectrEngInform 10(1):390–403
7. Sharif M, Amin J, Siddiqa A, Khan HU, Arshad Malik MSA, Anjum MA, Kadry S (2020) Recognition of different types of leukocytes using YOLOv2 and optimized bag-of-features. IEEE Access 8:167448–167459. https://doi.org/10.1109/ACCESS.2020.3021660
8. Rajinikanth V, Joseph Raj AN, Thanaraj KP, Naik GR (2020) A customized VGG19 network with concatenation of deep and handcrafted features for brain tumor detection. Appl Sci 10(10):3429. https://doi.org/10.3390/app10103429
9. Badrinarayanan V, Handa A, Cipolla R (2015) Segnet: A deep convolutional encoder-decoder architecture for robust semantic pixel-wise labelling. arXiv preprint arXiv:1505.07293
10. Badrinarayanan V, Kendall A, Cipolla R (2017) Segnet: a deep convolutional encoder-decoder architecture for image segmentation. IEEE Trans Pattern Anal Mach Intell 39(12):2481–2495. https://doi.org/10.1109/TPAMI.2016.2644615
11. El Adoui M, Mahmoudi SA, Larhmam MA, Benjelloun M (2019) MRI breast tumor segmentation using different encoder and decoder CNN architectures. Computers 8(3):52. https://doi.org/10.3390/computers8030052
12. Ronneberger O, Fischer P, Brox T (2015) U-net: convolutional networks for biomedical image segmentation. Lecture Notes in Computer Science International Conference on Medical Image Computing and Computer-Assisted Intervention, pp 234–41. https://doi.org/10.1007/978-3-319-24574-4_28
13. Fawakherji M, Youssef A, Bloisi D, Pretto A, Nardi D (2019) Crop and weeds classification for precision agriculture using context-independent pixel-wise segmentation. In: Third IEEE International Conference on Robotic Computing (IRC), IEEE Publications 2019, pp 146–152. https://doi.org/10.1109/IRC.2019.00029
14. Pravitasari AA, Iriawan N, Almuhayar M, Azmi T, Irhamah I, Fithriasari K, Purnami SW, Ferriastuti W (2020) UNet-VGG16 with transfer learning for MRI-based brain tumor segmentation. Telkomnika 18(3):1310–1318. https://doi.org/10.12928/telkomnika.v18i3.14753
15. Iglovikov V, Shvets A (2018) Ternausnet: U-net with VGG11 encoder pre-trained on imagenet for image segmentation. arXiv preprint arXiv:1801.05746
16. Frid-Adar M, Ben-Cohen A, Amer R, Greenspan H (2018) Improving the segmentation of anatomical structures in chest radiographs using U-Net with an imagenet pre-trained encoder. Lecture Notes in Computer Science, pp159–168. https://doi.org/10.1007/978-3-030-00946-5_17
17. Iglovikov V, Seferbekov SS, Buslaev A, Shvets A (2018) TernausNetV2: fully convolutional network for instance segmentation. CVPR Workshops p 233. https://doi.org/10.1109/CVPRW.2018.00042
18. http://users.cecs.anu.edu.au/~hrezatofighi/Data/Leukocyte%20Data.htm
19. Rezatofighi SH, Khaksari K, Soltanian-Zadeh H (2010) Automatic recognition of five types of white blood cells in peripheral blood. International Conference Image Analysis and Recognition, pp 161–172. https://doi.org/10.1007/978-3-642-13775-4_17
20. Rezatofighi SH, Soltanian-Zadeh H (2011) Automatic recognition of five types of white blood cells in peripheral blood. ComputMed ImagingGraph 35(4):333–343. https://doi.org/10.1016/j.compmedimag.2011.01.003
21. Alam MM, Islam MT (2019) Machine learning approach of automatic identification and counting of blood cells. Healthc Technol Lett 6(4):103–108. https://doi.org/10.1049/htl.2018.5098
22. Vatathanavaro S, Tungjitnob S, Pasupa K White blood cell classification: a comparison between VGG-16 and ResNet-50 models
23. Jung C, Abuhamad M, Alikhanov J, Mohaisen A, Han K, Nyang D (2019) W-net: a CNN-based architecture for white blood cells image classification. arXiv preprint arXiv:1910.01091
24. Prinyakupt J, Pluempitiwiriyawej C (2015) Segmentation of white blood cells and comparison of cell morphology by linear and naïve Bayes classifiers. Biomed Eng OnLine 14(1):63. https://doi.org/10.1186/s12938-015-0037-1
25. Almezhghwi K, Serte S (2020) Improved classification of white blood cells with the generative adversarial network and deep convolutional neural network. Comput Intell Neurosci 2020:6490479. https://doi.org/10.1155/2020/6490479

26. Li J, Wu J (2020) Leukocyte detection in blood smear image based on improved YOLOv3. In: Proceedings of the 2020 the 10th International Workshop on Computer Science and Engineering (WCSE 2020), pp 144–149. https://doi.org/10.18178/wcse.2020.06.024
27. Kutlu H, Avci E, Özyurt F (2020) White blood cells detection and classification based on regional convolutional neural networks. Med Hypotheses 135:109472. https://doi.org/10.1016/j.mehy.2019.109472
28. Dey N, Shi F, Rajinikanth V (2019) Leukocyte nuclei segmentation using entropy function and Chan-Vese approach. Inf Technol Intell Transp Syst 314: 255–264.. https://doi.org/10.3233/978-1-61499-939-3-255
29. Raja NSM, Arunmozhi S, Lin H, Dey N, Rajinikanth V (2019) A study on segmentation of leukocyte image with Shannon's entropy. Adv Med Technol Clin Pract pp 1–27. https://doi.org/10.4018/978-1-5225-6316-7.ch001
30. Rajinikanth V, Dey N, Kavallieratou E, Lin H (2020) Firefly algorithm-based Kapur's thresholding and Hough transform to extract leukocyte section from hematological images. Springer Tracts in Nature-Inspired Computing, pp 221–235. https://doi.org/10.1007/978-981-15-0306-1_10
31. Sapna S, Renuka A (2017) Techniques for segmentation and classification of leukocytes in blood smear images-a review. In: IEEE International Conference on Computational Intelligence and Computing Research (ICCIC). Vol. 2017. IEEE Publications; 2017, December. pp 1–5. https://doi.org/10.1109/ICCIC.2017.8524465
32. Song H, Han X-Y, Montenegro-Marin CE, Krishnamoorthy S (2021) Secure prediction and assessment of sports injuries using deep learning based convolutional neural network. J Ambient Intell Hum Comput 12(3):3399–3410. https://doi.org/10.1007/s12652-020-02560-4
33. Bobadilla J, Ortega F, Gutiérrez A, Alonso S (2020) Classification-based deep neural network architecture for collaborative filtering recommender systems. Int J Interact Multimedia Artif Intell 6(1):68–77. https://doi.org/10.9781/ijimai.2020.02.006
34. Lin JCW, Shao Y, Djenouri Y, Yun U (2021) ASRNN: a recurrent neural network with an attention model for sequence labeling. Knowl Based Syst 212:106548. https://doi.org/10.1016/j.knosys.2020.106548
35. Maheshan MS, Harish BS, Nagadarshan N (2020) A convolution neural network engine for sclerare cognition. Int J Interact Multimedia Artif Intell 6(1):78–83. https://doi.org/10.9781/ijimai.2019.03.006
36. https://www.kaggle.com/surajiiitm/bccd-dataset
37. https://www.kaggle.com/nikhilsharma00/leukemia-dataset
38. Donida Labati R, Piuri V, Scotti F (2011) ALL-IDB: the acute lymphoblastic leukemia image database for image processing. In: Proceedings of the 2011 IEEE International Conference on Image Processing (ICIP 2011), Brussels, Belgium, pp 2045–2048. https://doi.org/10.1109/ICIP.2011.6115881
39. Scotti F (2006) Robust segmentation and measurements techniques of white cells in blood microscope images. In: Proceedings of the 2006 IEEE Instrumentation and Measurement Technology Conference (IMTC 2006), Sorrento, Italy, pp 43–48. https://doi.org/10.1109/IMTC.2006.328170
40. Kasihmuddin MSBM, Mansor MAB, Abdulhabib Alzaeemi S, Sathasivam S (2021) Satisfiability logic analysis via radial basis function neural network with Artificial Bee Colony Algorithm. Int J Interact Multimedia Artif Intell 6(6):164–173. https://doi.org/10.9781/ijimai.2020.06.002
41. Devi SS, Singh NH, Laskar RH (2020) Fuzzy C-means clustering with histogram based cluster selection for skin lesion segmentation using non-dermoscopic images. Int J Interact Multimedia Artif Intell 6(1):26–31. https://doi.org/10.9781/ijimai.2020.01.001
42. Khari M, Garg AK, Gonzalez-Crespo RG, Verdú E (2019) Gesture recognition of RGB and RGB-D staticimages using convolutional neuralnetworks. Int J Interact Multimedia Artif Intell 5(7):22–27. https://doi.org/10.9781/ijimai.2019.09.002
43. Robinson YH, Vimal S, Khari M, Hernández FCL, Crespo RG (2020) Tree-based convolutional neural networks for object classification in segmented satellite images. Int J High Perform Comput Appl. https://doi.org/10.1177/1094342020945026
44. Pugalenthi R, Rajakumar MP, Ramya J, Rajinikanth V (2019) Evaluation and classification of the brain tumor MRI using machine learning technique. Control Eng Appl Inform 21(4):12–21
45. Dey N, Rajinikanth V, Shi F, Tavares JMRS, Moraru L, Arvind Karthik KA, Lin H, Kamalanand K, Emmanuel C (2019) Social-Group-Optimization based tumor evaluation tool for clinical brain MRI of Flair/diffusion-weighted modality. Biocybern Biomed Eng 39(3):843–856. https://doi.org/10.1016/j.bbe.2019.07.005
46. Wang Y, Chen Y, Yang N, Zheng L, Dey N, Ashour AS, Rajinikanth V, Tavares JMRS, Shi F (2019) Classification of mice hepatic granuloma microscopic images based on a deep convolutional neural network. Appl Soft Comput 74:40–50. https://doi.org/10.1016/j.asoc.2018.10.006

47. Mani MS, Manisha S, Thanaraj KP, Rajinikanth V (2017) Automated segmentation of Giemsa stained microscopic images based on entropy value. In: International Conference on Intelligent Computing, Instrumentation and Control Technologies (ICICICT). IEEE Publications; 2017, pp. 1124–1128. https://doi.org/10.1109/ICICICT1.2017.8342727
48. Wickham H, Hofmann H, Wickham C, Cook D (2012) Glyph-maps for visually exploring temporal patterns in climate data and models. Environmetrics 23(5):382–393. https://doi.org/10.1002/env.2152

Authors and Affiliations

Seifedine Kadry[1] · Venkatesan Rajinikanth[2] · David Taniar[3] · Robertas Damaševičius[4] · Xiomara Patricia Blanco Valencia[5]

Seifedine Kadry
Seifedine.kadry@noroff.no

Venkatesan Rajinikanth
v.rajinikanth@ieee.org

David Taniar
David.Taniar@monash.edu

Robertas Damaševičius
robertas.damasevicius@ktu.lt

1 Faculty of Applied Computing and Technology, Noroff University College, Kristiansand, Norway

2 Department of Electronics and Instrumentation Engineering, St. Joseph's College of Engineering, OMR, Tamil Nadu, Chennai 600119, India

3 Faculty of Information Technology, Monash University, Clayton Campus, Melbourne, VIC 3800, Australia

4 Faculty of Applied Mathematics, Silesian University of Technology, 44-100, Gliwice, Poland

5 Computer Science and Technology Area, Universidad Internacional de La Rioja (UNIR), Logroño, Spain